

# Phase-modulated electromagnetically induced transparency in a giant-atom system within waveguide QED

Wei Zhao,<sup>1</sup> Yan Zhang,<sup>1</sup> and Zihai Wang<sup>1,\*</sup>

<sup>1</sup>*Center for Quantum Sciences and School of Physics,  
Northeast Normal University, Changchun 130024, China*

(Dated: December 23, 2024)

The nonlocal emitter-waveguide coupling, which gives birth to the so called giant atom, represents a new paradigm in the field of quantum optics and waveguide QED. In this paper, we investigate the single-photon scattering in a one-dimensional waveguide on a two-level or three-level giant atom. Thanks to the natural interference induced by the back and forth photon transmitted/reflected at the atom-waveguide coupling points, the photon transmission can be dynamically controlled by the periodic phase modulation via adjusting the size of the giant atom. For the two-level giant-atom setup, we demonstrate the energy shift which is dependent on the atomic size. For the driven three-level giant-atom setup, it is of great interest that, the interference effect between different atomic transition paths, can lead to a complete transmission window, analogous to the electromagnetically induced transparency and beyond the two-photon resonance mechanism, and the width of the transmission valleys (reflection range) is tunable in terms of the atomic size. Our investigation will be beneficial to the photon or phonon control in quantum network based on mesoscopical or even macroscopical quantum nodes involving the giant atom.

## I. INTRODUCTION

In the field of quantum optics, the study of the interaction between light and matter is one of the long-lived subjects. Recently, the light-matter interaction in waveguide structures has attracted much attention, which leads to lots of theoretical and experimental works in waveguide QED community [1–6], such as dressed or bound states [7–12], phase transitions [13, 14], single-photon devices [15–17], exotic topological and chiral phenomena [18–23], where the wavelength of light (or microwave field) is usually tens or hundreds of times larger than the size of the natural/artificial atoms constituting the matter [24–28]. Therefore, the light-matter interaction is usually modelled by the dipole approximation, where the atoms are regarded as point-like dipoles [29].

However, in recent years, the artificial superconducting transmon qubit coupled by the acoustic waves [30–32], of which the size is comparable to the wavelength of the phonons, is named as “giant atom” and has been successfully realized in experiments [33]. Alternatively, the giant-atom model can also be realized in the superconducting transmission line setup, where the capacitive or inductive coupling allows more than one coupling points between the microwave field and the qubit [34, 35]. Moreover, using the cold atomic system, a theoretical scheme for the realization of giant atom has been proposed in dynamical state-dependent optical lattices [36]. In the giant-atom community, a lot of new phenomena not existing in the conventional small atomic system have been predicted, such as frequency dependent relaxation [37], non-exponential decay [38–40], tunable bound state [41, 42] as well as decoherence free subspace [43, 44]

(For a recent review, see Ref. [45]). The underlying physics behind these phenomena is the interference and retarded effect during the photon/phonon propagating process between the different coupling points.

On the other hand, the dynamical control of the single-photon transmission is a hot topic in constructing quantum networks [46–48], motivated by the photon based quantum information processing. Photons provide a reliable transmission of quantum information and the waveguide is often seen as photonic channels in quantum network, with atoms (or artificial atoms) acting as quantum nodes. Along this line, people have proposed lots of schemes to realize single-photon device, in which the propagating of the photon in channels is controlled on demand by adjusting the nature of the quantum nodes [15–17, 49–53]. Combined with the interference effect, it motivates us to study how to modulate the single photon scattering by the giant atom.

In this paper, we tackle this issue in a one-dimensional waveguide with a two-level or three-level giant atom. For the two-level atom setup, we find that the change in the size of the atom can control its energy shift due to the interference effect between the backward and forward photon in the waveguide. In the driven three-level giant-atom system, we demonstrate the controllable phase-modulated electromagnetically induced transparency (EIT) [54–58] physics, which also arises from and can be controlled by the incorporation of the two interference effects induced by the interplay of the photon transmissions and atomic transitions, respectively. And then, the size of the giant atom, which serves as a controller, can be used to tune the width of the transmission valleys (reflection) in a periodical manner. The underlying physical principal is further revealed in the viewpoint of quantum open system based on the dressed state representation.

The rest of the paper is structured as follows: In Sec. II,

\* wangzh761@nenu.edu.cn

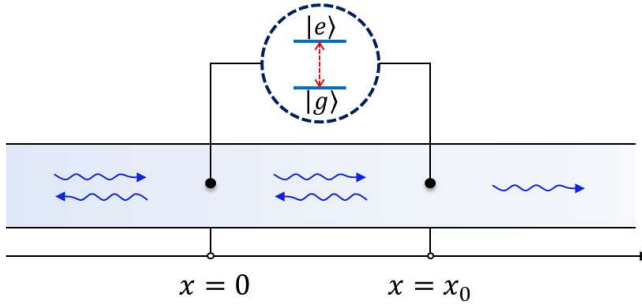


FIG. 1. Schematic configuration for a linear waveguide coupled to a giant atom at the points  $x = 0$  and  $x = x_0$ .

we present the model and discuss the single photon scattering in a two-level giant-atom system. In Sec. III, we demonstrate the EIT scattering behavior for a driven three-level giant-atom with  $\Lambda$ -type transition. At last, we end up with a brief conclusion in Sec. IV.

## II. TWO-LEVEL GIANT ATOM

As schematically shown in Fig. 1, the system we consider is composed of a linear waveguide and a giant atom, which is actually a two-level system. The giant atom is connected to the waveguide via two points with  $x = 0$  and  $x = x_0$ , respectively. The Hamiltonian  $H_1$  of the system can be divided into three parts, i.e.,  $H_1 = H_s + H_\omega + V_1$ . The first part  $H_s$  is the free Hamiltonian of the giant atom (Hereafter, we set  $\hbar = 1$ ).

$$H_s = \omega_e |e\rangle\langle e|, \quad (1)$$

where  $\omega_e$  is the transition frequency between the ground state  $|g\rangle$  and the excited state  $|e\rangle$ .

The second part  $H_\omega$  of the Hamiltonian  $H_1$  represents the free Hamiltonian of the waveguide, and is expressed as

$$H_\omega = \int dx \left\{ -iv_g C_R^\dagger(x) \frac{d}{dx} C_R(x) + iv_g C_L^\dagger(x) \frac{d}{dx} C_L(x) \right\}, \quad (2)$$

where  $v_g$  is the group velocity of photons traveling in the waveguide. Here, we assume that the group velocity possesses the same unit as the frequency by considering the length of the waveguide to be dimensionless.  $C_R^\dagger(x)[C_L^\dagger(x)]$  is the bosonic creation operator for the right-going (left-going) photon at position  $x$ .

For the third part  $V_1$  of the Hamiltonian  $H_1$ , we describe the interaction between the waveguide and the giant atom. Within the rotating wave approximation, the

Hamiltonian  $V_1$  can be expressed as

$$V_1 = f \int dx \delta(x) [\sigma^+ C_R(x) + \sigma^+ C_L(x) + \text{H.c.}] + f \int dx \delta(x - x_0) [\sigma^+ C_R(x) + \sigma^+ C_L(x) + \text{H.c.}], \quad (3)$$

where  $f$  is the coupling strength between the waveguide and the two-level giant atom.  $\sigma^+ = (\sigma^-)^\dagger = |e\rangle\langle g|$  is the raising operator of the atom. The Dirac- $\delta$  function in the Hamiltonian  $V_1$  indicates that the giant atom has a length of  $x_0$  and connects to the waveguide via its head and tail, that is,  $x = 0$  and  $x = x_0$ .

It is noted that, the total excitation of the atom and the photon in the waveguide is conserved. In the following section, we will restrict ourselves in the single excitation subspace, to investigate how to control the single photon scattering state via adjusting the frequency of the photon and the size of the two-level giant atom.

In the single-excitation subspace, the eigenstate of the system can be written as

$$|E\rangle = \int dx \left[ \phi_{R_1}(x) C_R^\dagger(x) + \phi_{L_1}(x) C_L^\dagger(x) \right] |G\rangle + u_e \sigma^+ |G\rangle, \quad (4)$$

where  $|G\rangle$  represents that the waveguide is in the vacuum states while the giant atom is in the ground state  $|g\rangle$ .  $\phi_{R_1}(x)$  and  $\phi_{L_1}(x)$  are single-photon wave functions of the right-going and left-going modes in the waveguide, respectively.  $u_e$  is the excitation amplitude of the giant atom. Solving the stationary Schrödinger equation  $H_1 |E\rangle = E |E\rangle$ , the amplitudes equation can be obtained as

$$-iv_g \frac{d}{dx} \phi_{R_1}(x) + fu_e M = E \phi_{R_1}(x), \quad (5a)$$

$$iv_g \frac{d}{dx} \phi_{L_1}(x) + fu_e M = E \phi_{L_1}(x), \quad (5b)$$

$$w_e u_e + f N = E u_e. \quad (5c)$$

where  $M = \delta(x) + \delta(x - x_0)$  and  $N = \phi_{R_1}(0) + \phi_{R_1}(x_0) + \phi_{L_1}(0) + \phi_{L_1}(x_0)$ .

Next, we consider the scattering behavior when a single photon with wave vector  $k$  is incident from the left side of the waveguide. In this case, the wave function of  $\phi_{R_1}(x)$  and  $\phi_{L_1}(x)$  can be expressed as

$$\phi_{R_1}(x) = e^{ikx} \{ \theta(-x) + A_1 [\theta(x) - \theta(x - x_0)] + t_1 \theta(x - x_0) \}, \quad (6)$$

$$\phi_{L_1}(x) = e^{-ikx} \{ r_1 \theta(-x) + B_1 [\theta(x) - \theta(x - x_0)] \}, \quad (7)$$

with

$$\theta(x) = \begin{cases} 1 & x > 0 \\ \frac{1}{2} & x = 0 \\ 0 & x < 0 \end{cases}. \quad (8)$$

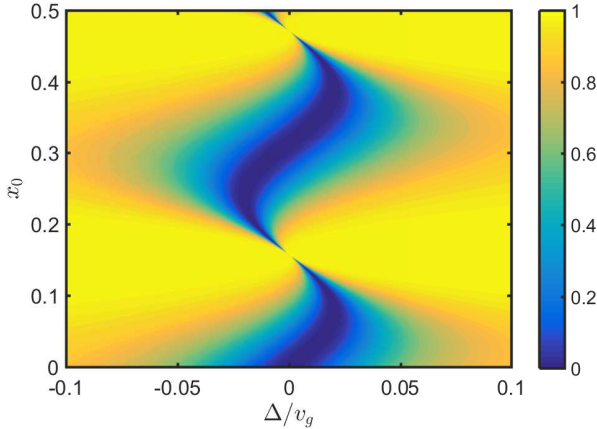


FIG. 2. The transmission rate  $T_1$  as functions of  $x_0$  and  $\Delta$ . The parameters are set as  $\omega_e/v_g = 20, f/v_g = 0.1$ .

We explain the expression of the above wave functions physically as follows. When the right-going photon incident from the region  $x < 0$  reaches the first connection point  $x = 0$  between the giant atom and the waveguide, it can be transmitted or reflected, with the amplitudes of  $A_1$  and  $r_1$ , respectively. The photon transmitted at the first connection point at  $x = 0$  will travel freely in the waveguide until it reaches the second connection point at  $x = x_0$ , it will be then reflected or transmitted secondly, with the amplitudes  $B_1$  and  $t_1$ , respectively.

Now, we substitute Eqs. (6-8) into the amplitude Eqs. (5), it yields the dispersion relation  $E = v_g k$ . Furthermore, the transmission rate  $T_1 = |t_1|^2$  can be obtained as

$$T_1 = \frac{(\Delta v_g - 2f^2 \sin kx_0)^2}{(\Delta v_g - 2f^2 \sin kx_0)^2 + 4f^4 (1 + \cos kx_0)^2}, \quad (9)$$

where  $\Delta = E - \omega_e$  is the detuning between the atom and the propagating photon in the waveguide.

In the small atom scenario ( $x_0 = 0$ ) which is studied in Ref. [15], it is obvious that the incident photon will be completely reflected ( $T_1 = 0$ ) when it is resonant with the atom, that is,  $\Delta = 0$ . However, for the giant atom in our setup, the incident photon will propagate back and forth in the spatial regime covered by the giant atom, leading to an interference effect. As a result, as shown in Fig. 2, the transmission rate can be controlled by adjusting the photon-atom detuning  $\Delta$  and the size of the giant atom  $x_0$ . Interestingly, in the giant-atom situation ( $x_0 \neq 0$ ), the detuning for complete reflection is determined by the transcendental equation

$$\Delta_r = \frac{2f^2 \sin k_r x_0}{v_g}, \quad (10)$$

where  $\Delta_r$  is dependent on  $k_r$  via  $\Delta_r = v_g k_r - \omega_e$ . Since the atomic frequency is implied by the location of the

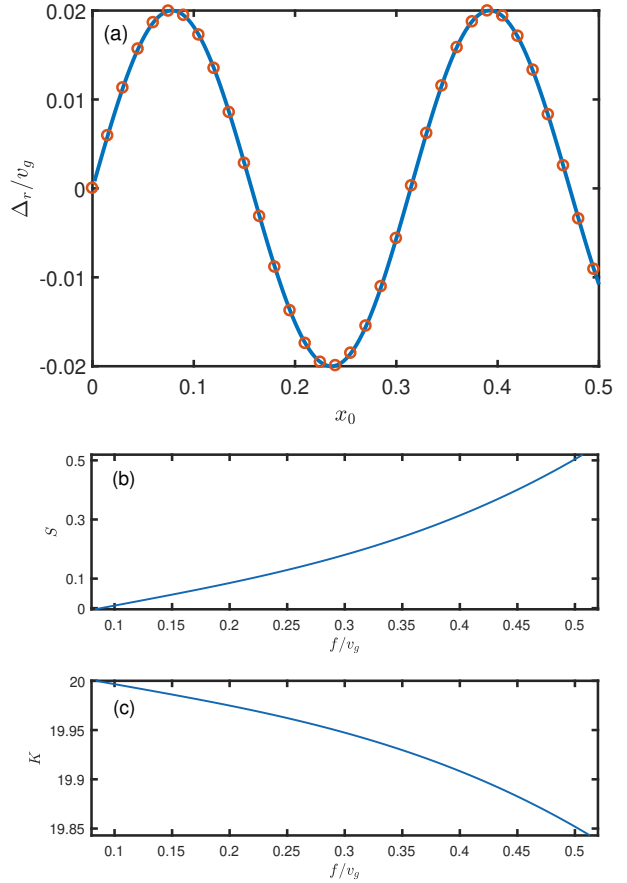


FIG. 3. (a) The detuning  $\Delta_r$  as a function of  $x_0$  for  $f/v_g = 0.1$ . The solid line is given by the solution of the transcendental equation in Eq. (10) and the empty circles are the results from the numerical fitting. (b) and (c) The fitting parameters  $S$  and  $K$  in Eq. (11) as a function of the atom-waveguide coupling strength  $f$ . In all of the panels, the atomic transition frequency is set to be  $\omega_e/v_g = 20$ .

complete reflection of the incident photon [15], we can observe an atomic frequency shift which originates from the interference effect as discussed above, compared with the small atom system. It implies that, only when the frequency of the incident photon satisfies  $|\Delta_r| \leq 2f^2/v_g$ , that is,  $\omega_e + 2f^2/v_g \geq v_g k_r \geq \omega_e - 2f^2/v_g$ , it is possible to be completely reflected. Within this regime, we plot the dependence of  $\Delta_r$  on the size of giant atom  $x_0$  in Fig. 3(a) (solid line), which shows a sinusoidal shape. The exact sinusoidal shape by the numerical fitting (empty circles) is also shown in the figure and the fitting function is obtained by

$$\Delta_r \approx S \sin(Kx_0), \quad (11)$$

where the fitting parameters  $S \approx 2f^2/v_g$  and  $K$  are plotted as a function of atom-waveguide coupling strength  $f$  in Fig. 3(b) and (c), respectively. For the weak coupling, it shows that  $K$  is nearly equal to  $\omega_e/v_g$  ( $\omega_e/v_g = 20$

in our consideration) and gradually diverges from it in a quadratic manner. Therefore, the energy shift of the giant atom can be larger than its natural line width (not considered in this paper) and observed experimentally by increasing the atom-waveguide coupling strength.

### III. THREE-LEVEL GIANT ATOM

In this section, let us consider the single-photon scattering on a driven  $\Lambda$ -type three-level giant atom. As schematically shown in Fig. 4, the atom is characterized by the ground state  $|g\rangle$ , excited state  $|e\rangle$  and metastable state  $|f\rangle$ . Here, there are two types of interference channels. One is similar to that in two-level giant atom system, that is, the interplay between the multiple backward and forward photons of the transmission and reflection in the waveguide; the other is peculiar for such a three-level EIT atomic system, that is, the interference between two transition paths  $|g\rangle \rightarrow |e\rangle$  and  $|g\rangle \rightarrow |e\rangle \rightarrow |f\rangle \rightarrow |e\rangle$ . The incorporation between two interference channels may provide a possibility of the extra and interesting property of the giant-atom EIT effect.

The Hamiltonian  $H_2$  of the current system can be divided into three parts, i.e.,  $H_2 = H_w + H_a + V_2$ . Here,  $H_w$  is the free Hamiltonian of the waveguide which is given in Eq. (2).  $H_a$  is the Hamiltonian of the giant atom

$$H_a = \omega_e |e\rangle \langle e| + \omega_f |f\rangle \langle f| + \eta (|e\rangle \langle f| e^{-i\omega_d t} + |f\rangle \langle e| e^{i\omega_d t}), \quad (12)$$

where  $\omega_e$  and  $\omega_f$  ( $\omega_f < \omega_e$ ) are the frequencies of the state  $|e\rangle$  and  $|f\rangle$ , respectively. As a reference, we have set  $\omega_g = 0$ .  $\eta$  and  $\omega_d$  are, respectively, the strength and frequency of the classical field, which drives  $|f\rangle \leftrightarrow |e\rangle$  transition. In the rotating frame, the time independent Hamiltonian becomes

$$\tilde{H}_a = \omega_e |e\rangle \langle e| + \delta |f\rangle \langle f| + \eta (|e\rangle \langle f| + |f\rangle \langle e|), \quad (13)$$

where  $\delta = \omega_f + \omega_d$ .

The third part  $V_2$  of the Hamiltonian  $H_2$  describes the interaction between the waveguide and the giant atom. Within the rotating wave approximation, it can be expressed as

$$V_2 = f \int dx \delta(x) \left\{ \left[ C_R^\dagger(x) + C_L^\dagger(x) \right] |g\rangle \langle e| + \text{H.c.} \right\} + f \int dx \delta(x - x_0) \left\{ \left[ C_R^\dagger(x) + C_L^\dagger(x) \right] |g\rangle \langle e| + \text{H.c.} \right\}, \quad (14)$$

where  $f$  is the coupling strength between the waveguide and giant atom.

In the single-excitation subspace, the eigenstate of the system can be expressed as

$$|E\rangle = \int dx \left[ \phi_{R_2}(x) C_R^\dagger + \phi_{L_2}(x) C_L^\dagger \right] |\emptyset, g\rangle + \lambda_e |\emptyset, e\rangle + \lambda_f |\emptyset, f\rangle, \quad (15)$$

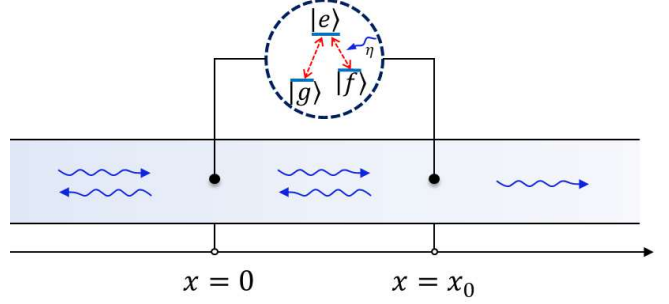


FIG. 4. Schematic configuration for a linear waveguide coupled to a  $\Lambda$ -type three-level giant atom at the points  $x = 0$  and  $x = x_0$ .

where  $|\emptyset, m\rangle$  ( $m = e, g, f$ ) represents that the waveguide is in the vacuum state while the giant atom is in the state  $|m\rangle$ .  $\phi_{R_2}(x)$  and  $\phi_{L_2}(x)$  are single-photon wave functions of the right-going and left-going modes in the waveguide, respectively.  $\lambda_e$  and  $\lambda_f$  are the excitation amplitudes of the giant atom in the excited state  $|e\rangle$  and metastable state  $|f\rangle$ , respectively. Similar to the discussion in two-level atom setup, for a right-going incident photon with wave vector  $k$ , the photon amplitude can be expressed as

$$\phi_{R_2}(x) = e^{ikx} \{ \theta(-x) + A_2 [\theta(x) - \theta(x - x_0)] + t_2 \theta(x - x_0) \}, \quad (16)$$

$$\phi_{L_2}(x) = e^{-ikx} \{ r_2 \theta(-x) + B_2 [\theta(x) - \theta(x - x_0)] \}, \quad (17)$$

where  $t_2$  and  $r_2$  are the transmission and reflection amplitudes while  $A_2$  ( $B_2$ ) are the amplitudes for finding a right (left)-going photon inside the regime of the giant atom. Then, the Schrödinger equation  $\tilde{H}|E\rangle = E|E\rangle$  (where  $\tilde{H} = H_w + \tilde{H}_a + V_2$ ) yields

$$t_2 = \frac{(E - \delta) [i(E - \omega_e) v_g - 2if^2 \sin(kx_0)] - iv_g \eta^2}{(E - \delta) [i(E - \omega_e) v_g - 2f^2 (1 + e^{ikx_0})] - iv_g \eta^2}, \quad (18)$$

$$r_2 = \frac{2f^2(E - \delta) (1 + \cos(kx_0)) e^{ikx_0}}{(E - \delta) [i(E - \omega_e) v_g - 2f^2 (1 + e^{ikx_0})] - iv_g \eta^2}. \quad (19)$$

Then the transmission rate  $T_2 = |t_2|^2$  and reflection rate  $R_2 = |r_2|^2$  satisfy  $T_2 + R_2 = 1$  due to the neglect of the natural relaxations in the atom.

In Fig. 5, we plot the transmission rate  $T_2$  as functions of the detuning  $\Delta = E - \omega_e$  between the incident photon and atomic  $|g\rangle \leftrightarrow |e\rangle$  transition and the size of the giant atom  $x_0$ . Here, we illustrate the result for resonantly driving the atom by the field  $\eta$  in Fig. 5(a) and (d), and non-resonantly in Fig. 5(b),(c) and (e). All of the results are characterized by two narrow transmission

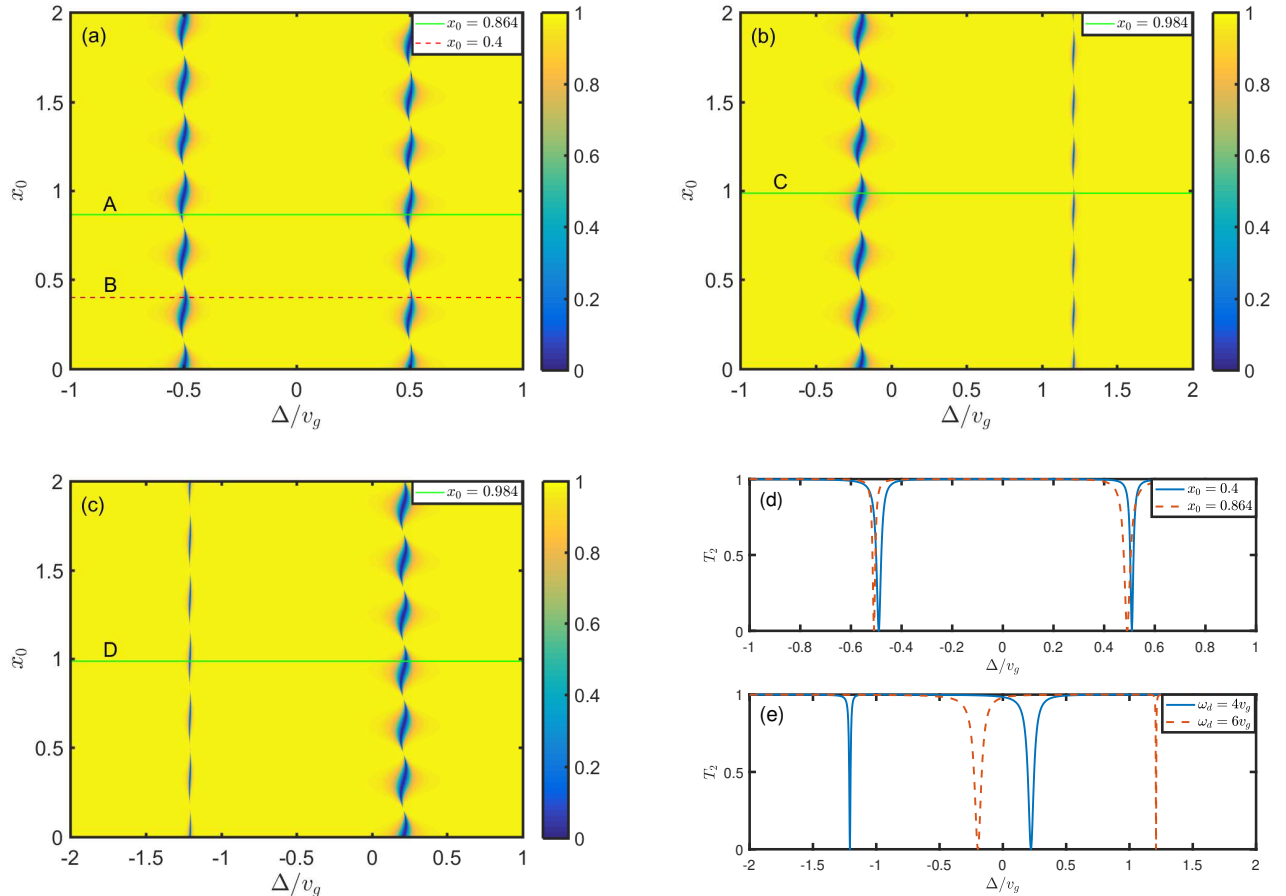


FIG. 5. The transmission rate  $T_2$  as functions of the detuning  $\Delta = E - \omega_e$  and the size of the giant atom  $x_0$  for resonant driving. The parameters are set as  $\omega_e/v_g = 20, \omega_f/v_g = 15, f/v_g = 0.1, \eta/v_g = 0.5$ . The other parameters are  $\omega_d/v_g = 5, \omega_d/v_g = 6, \omega_d/v_g = 4$  for (a), (b) and (c), respectively. (d) The rate  $T_2$  for the lines labelled by "A" (solid) and "B" (dashed) in (a). (e) The rate  $T_2$  for the line labelled by "C" (solid) and "D" (dashed) in (b) and (c), respectively.

valleys ( $T_2 \simeq 0$ ) and a relatively wide transmission windows ( $T_2 \simeq 1$ ) between them around the two-photon resonance.

First, we focus on the transmission window ( $T_2 \simeq 1, R_2 \simeq 0$ ). It can be observed in Eq. (19) that  $R_2=0$  when  $E - \delta = E - \omega_f - \omega_d = 0$ , which implies the two-photon resonance condition  $\omega_e - E = \omega_e - \omega_f - \omega_d$ . It is same to that in the small atom setup and the complete transmission is popularly regarded as induced by the destructive interference between the  $|g\rangle \rightarrow |e\rangle$  and  $|g\rangle \rightarrow |e\rangle \rightarrow |f\rangle \rightarrow |e\rangle$  transition paths. This is similar to the usual EIT phenomenon [54–57]. However, we did not consider the natural relaxations of the states  $|e\rangle$  and  $|f\rangle$ , therefore, the window (valley) here is much wider (narrower) than that widely studied in EIT. Moreover, we can also observe that  $R_2 = 0$  when  $1 + \cos kx_0 = 0$ , that is  $kx_0 = (2m + 1)\pi$  where  $m$  is an integer, and the dependence of the position is peculiar for the giant atom setup. Note that  $kx_0$  is the accumulated phase as the travelling photon moves from one coupling point to the other. Therefore, such a EIT-like transmission is also re-

lated to the position-dependent phase introduced by the interference effect from the back and forth photons inside the regime covered by the giant atom. Next, we discuss the two valleys, which represent the complete reflection ( $T_2 \simeq 0, R_2 \simeq 1$ ). Based on Eq. (18), the complete reflection occurs when

$$E_{\pm} = \omega_e + f^2 \sin(kx_0)/v_g - \frac{\Delta_2}{2} \pm \frac{\sqrt{(\Delta_2 + 2f^2 \sin(kx_0)/v_g)^2 + 4\eta^2}}{2}, \quad (20)$$

where  $\Delta_2 = \omega_e - \omega_f - \omega_d$  is the detuning between the driving field and the atomic  $|f\rangle \leftrightarrow |e\rangle$  transition. This fact can be explained intuitively in the dressed state presentation. The eigenfrequencies of the driving Hamiltonian  $\tilde{H}_a$  in Eq. (13) are

$$\omega_{\pm} = \omega_e - \frac{\Delta_2}{2} \pm \frac{\sqrt{\Delta_2^2 + 4\eta^2}}{2}. \quad (21)$$

TABLE I. The values of  $x_0$ ,  $\Delta_2$  and corresponding values of  $|G_{\pm,k}|$  for the two valleys in Fig. 5 (d) and (e).

Line Label	curve	$\Delta_2/v_g$	$x_0$	$f G_{-, \omega_- / v_g} /v_g$	$f G_{+, \omega_+ / v_g} /v_g$
A	solid in Fig. 5(d)	0	0.4	1.4519	1.1496
B	dashed in Fig. 5(d)	0	0.864	1.0793	1.6851
C	dashed in Fig. 5(e)	-1	0.984	1.7558	0.4099
D	solid in Fig. 5(e)	1	0.984	0.7573	1.6093

and the corresponding states are

$$|\psi_+\rangle = \cos \frac{\theta}{2} |e\rangle + \sin \frac{\theta}{2} |f\rangle, \quad (22)$$

$$|\psi_-\rangle = -\sin \frac{\theta}{2} |e\rangle + \cos \frac{\theta}{2} |f\rangle. \quad (23)$$

For the resonantly driving ( $\Delta_2 = 0$ ), we will have  $\theta = \pi/2$ . For the case of non-resonantly driving, we will have  $\theta = \text{atan}(2\eta/\Delta_2)$  for  $\Delta_2 > 0$  and  $\theta = \pi + \text{atan}(2\eta/\Delta_2)$  for  $\Delta_2 < 0$ .

Comparing Eq. (21) with (20), we find that the incident photon will be completely reflected when it is “nearly” resonant with  $\omega_{\pm}$ . This fact is verified by the results shown in Fig. 5. Here, we use the phrase “nearly” to imply that  $E_{\pm}$  is not exactly equal to  $\omega_{\pm}$ , but is slightly modulated by  $x_0$ . As a result, the photon transmission shows a periodic phase modulation in terms of  $x_0$ , which is clearly demonstrated in Figs. 5 (a), (b) and (c) for both of resonantly and non-resonantly driving situations.

It is also shown in Fig. 5 that the two valleys discussed above possess different widths. For example, see the horizontal lines labelled by “A”, “B”, “C” and “D” in Figs. 5 (a), (b) and (c). This can be explained by the different effective decay rates of the eigenstates with frequency  $\omega_{\pm}$  in the viewpoint of quantum open system by regarding the waveguide as the effective environment. To this end, we rewrite the interaction Hamiltonian  $V_2$  in the momentum space by performing the Fourier transformation (in terms of  $|\psi_{\pm}\rangle$ ) as

$$V_2 = \sum_k \{ [C_L^\dagger(k) + C_R^\dagger(k)] |g\rangle [G_{+,k} \langle \psi_+ | + G_{-,k} \langle \psi_- |] + \text{H.c.} \} \quad (24)$$

where

$$G_{+,k} = f \cos \frac{\theta}{2} (1 + e^{ikx_0}), \quad G_{-,k} = -f \sin \frac{\theta}{2} (1 + e^{ikx_0}), \quad (25)$$

characterize the coupling strength between the  $k$ th mode in the waveguide and the giant atom. We note that,  $|G_{+,k}|$  and  $|G_{-,k}|$  actually reflect the width of the two valleys when the value of  $k$  is taken to satisfy  $v_g k = \omega_{\pm}$ .

In Table I, we list the values of  $|G_{+,k}|$  and  $|G_{-,k}|$  for the horizontal lines in Fig. 5(a) (b) and (c), along which the transmission rates are plotted as functions of the detuning  $\Delta$  in Fig. 5 (d) and (e). It shows a good agreement for the valley width between the table and the curves. For the resonant driving, which valley is wider depends on

the size of the giant atom  $x_0$ , as shown in Fig. 5 (a) and (d). However, for the non-resonant driving, as shown in Fig 5 (c), (c) and (e), the left valley is nearly always narrower than the right one when  $\Delta_2 > 0$  and wider when  $\Delta_2 < 0$ . In this sense, the modification to the photon transmission by the atomic size is more sensitive for the resonant driving setup.

#### IV. CONCLUSION

In this paper, we have studied the single-photon transmission in a one-dimensional linear waveguide system coupled with two-level or three-level giant atom. Generally, in the giant-atom regime, the backward and forward photons propagating in the waveguide can lead to an interference effect. Thus, for the case of two-level giant atom, we have shown that the complete reflection occurs, but not for the case that the incident photon is exactly resonant to the atom. In other words, the natural interference leads to an effective small but nonzero frequency shift, and the shift can be approximately regarded as a sinusoidal function of the atomic size. For the driven three-level giant atom, with the other interference channel induced by the two different atomic transition paths, we obtain a EIT-like line shape; more, with the incorporation between these two interference channels, the transparency window can be controlled by phase modulation in terms of the size of the atom. Also, the location and width of the transmission valleys are tunable by adjusting the atomic size.

Beyond the specific model here, our work demonstrates how to use the interplay between (among) the different interference channels to modify the photon transmission in the waveguide. In the giant atom scenario, one of the interference channels is provided by the photon propagation, while the other arises from the atomic transitions. Motivating by the interplay mechanism, we hope that the giant atom can be useful in designing photon or phonon based quantum device, which goes beyond the conventional small atom setup.

#### ACKNOWLEDGMENTS

This work is supported by National Natural Science Foundation of China (Grant No. 11875011, No. 12047566) and the Fundamental Research Funds for the Central Universities (Grant No. 2412019FZ045).

---

[1] X. Gu, A. F. Kockum, A. Miranowicz, Y.-x. Liu and F. Nori, Phys. Rep. **718**, 1 (2017).

[2] D. Roy, C. M. Wilson and O. Firstenberg, Rev. Mod. Phys. **89**, 021001 (2017).

[3] G.-Z. Song, E. Munro, W. Nie, F.-G. Deng, G.-J. Yang and L.-C. Kwek, Phys. Rev. A **96**, 043872 (2017).

[4] G.-Z. Song, E. Munro, W. Nie, L.-C. Kwek, F.-G. Deng and G.-L. Long, Phys. Rev. A **98**, 023814 (2018).

[5] G.-Z. Song, L.-C. Kwek, F.-G. Deng and G.-L. Long, Phys. Rev. A **99**, 043830 (2019).

[6] I. Iorsh, A. Poshakinskiy and A. Poddubny, Phys. Rev. Lett. **125**, 183601 (2020).

[7] H. Zheng, D. J. Gauthier and H. U. Baranger, Phys. Rev. A **82**, 063816 (2010).

[8] T. Shi, Y.-H. Wu, A. González-Tudela and J. I. Cirac, Phys. Rev. X **6**, 021027 (2016).

[9] G. Calajó, F. Ciccarello, D. Chang and P. Rabl, Phys. Rev. A **93**, 033833 (2016).

[10] E. Sánchez-Burillo, D. Zueco, L. Martín-Moreno and J. J. G.-Ripoll, Phys. Rev. A **96**, 023831 (2017).

[11] P. T. Fong and C. K. Law, Phys. Rev. A **96**, 023842 (2017).

[12] G. Calajó, Y.-L. L. Fang, H. U. Baranger and F. Ciccarello, Phys. Rev. Lett. **122**, 073601 (2019).

[13] M. Fitzpatrick, N. M. Sundaresan, A. C. Y. Li, J. Koch and A. A. Houck, Phys. Rev. X **7**, 011016 (2017).

[14] L. Qiao, Y.-J. Song and C.-P. Sun, Phys. Rev. A **100**, 013825 (2019).

[15] J.-T. Shen and S. Fan, Phys. Rev. Lett. **95**, 213001 (2005).

[16] D. E. Chang, A. S. Sørensen, E. A. Demler and M. D. Lukin, Nature Phys. **3**, 807 (2007).

[17] L. Zhou, Z. R. Gong, Y.-x. Liu, C. P. Sun and F. Nori, Phys. Rev. Lett. **101**, 100501 (2008).

[18] M. Ringel, M. Pletyukhov and V. Gritsev, New J. Phys. **16**, 113030 (2014).

[19] V. Yannopapas, Int. J. Mod. Phys. B **28**, 1441006 (2014).

[20] C. G.-Ballester, E. Moreno, F. J. Garcia-Vidal and A. G.-Tudela, Phys. Rev. A **94**, 063817 (2016).

[21] I. M. Mirza and J. C. Schotland, Phys. Rev. A **94**, 012302 (2016).

[22] S. Mahmoodian, G. Calajó, D. E. Chang, K. Hammerer and A. S. Sørensen, Phys. Rev. X **10**, (2020).

[23] M. Bello, G. Platero, J. I. Cirac and A. G.-Tudela, Sci. Adv. **5**, eaaw0279 (2019).

[24] P. Goy, J. M. Raimond, M. Gross and S. Haroche, Phys. Rev. Lett. **50**, 1903 (1983).

[25] D. Leibfried, R. Blatt, C. Monroe and D. Wineland, Rev. Mod. Phys. **75**, 281 (2003).

[26] A. Wallraff, D. I. Schuster, A. Blais, L. Frunzio, R. S. Huang, J. Majer, S. Kumar, S. M. Girvin and R. J. Schoelkopf, Nature **431**, 162 (2004).

[27] R. Miller, T. E. Northup, K. M. Birnbaum, A. Boca, A. D. Boozer and H. J. Kimble, Journal of Physics B: Atomic, Molecular and Optical Physics **38**, S551 (2005).

[28] S. Haroche, Rev. Mod. Phys. **85**, 1083 (2013).

[29] D. Walls and G. J. Milburn, *Quantum Optics*, 2nd ed (Springer, 2018).

[30] S. Datta, *Surface Acoustic Wave Devices*, (Prentice-Hall, Englewood Cliffs, NJ, 1986).

[31] D. Morgan, *Surface Acoustic Wave Filters*, 2nd ed. (Academic, Amsterdam, 2007).

[32] R. Manenti, A. F. Kockum, A. Patterson, T. Behrle, J. Rahamim, G. Tancredi, F. Nori and P. J. Leek, Nat. Comm. **8**, 975 (2017).

[33] M. V. Gustafsson, T. Aref, A. F. Kockum, M. K. Ekström, G. Johansson and P. Delsing, Science **346**, 207 (2014).

[34] B. Kannan, M. Ruckriegel, D. Campbell, A. F. Kockum, J. Braumüller, D. K. Kim, M. Kjaer-gaard, P. Krantz, A. Melville, B. M. Niedzielski, A. Vepsäläinen, R. Winik, J. L. Yoder, F. Nori, T. P. Orlando, S. Gustavsson and W. D. Oliver, Nature **583**, 775 (2020).

[35] A. M. Vadiraj, A. Ask, T. G. McConkey, I. Nsanzineza, C. W. Sandbo Chang, A. F. Kockum and C. M. Wilson, arXiv:2003.14167 (2020).

[36] A. G.-Tudela, C. S. Muñoz and J. I. Cirac, Phys. Rev. Lett. **122**, 203603 (2019).

[37] A. Frisk Kockum, P. Delsing and G. Johansson, Phys. Rev. A **90**, 013837 (2014).

[38] L. Guo, A. Grimsmo, A. F. Kockum, M. Pletyukhov and G. Johansson, Phys. Rev. A **95**, 053821 (2017).

[39] G. Andersson, B. Suri, L. Guo, T. Aref and P. Delsing, Nat. Phys. **15**, 1123 (2019).

[40] S. Guo, Y. Wang, T. Purdy and J. Taylor, Phys. Rev. A **102**, 033706 (2020).

[41] L. Guo, A. F. Kockum, F. Marquardt and G. Johansson, Phys. Rev. Research **2**, 043014 (2020).

[42] X. Wang, T. Liu, A. F. Kockum, H.-R. Li and F. Nori, Phys. Rev. Lett. **126**, 043602 (2021).

[43] A. F. Kockum, G. Johansson and F. Nori, Phys. Rev. Lett. **120**, 140404 (2018).

[44] A. Carollo, D. Cilluffo and F. Ciccarello, Phys. Rev. Research **2**, 043184 (2020).

[45] A. F. Kockum, in International Symposium on Mathematics, Quantum Theory, and Cryptography, (Springer Singapore, Singapore, 2021), p. 125. [also see arXiv: 1912.13012 (2019)].

[46] H. J. Kimble, Nature **453**, 1023 (2008).

[47] S. Ritter, C. Nölleke, C. Hahn, A. Reiserer, A. Neuzner, M. Uphoff, M. Mücke, E. Figueroa, J. Bochmann and G. Rempe, Nature **484**, 195 (2012).

[48] P. Lodahl, Quantum Science and Technology **3**, 013001 (2017).

[49] J. T. Shen and S. Fan, Phys. Rev. A **79**, 023837 (2009).

[50] P. Longo, P. Schmitteckert and K. Busch, Phys. Rev. Lett. **104**, 023602 (2010).

[51] W.-B. Yan, J.-F. Huang and H. Fan, Sci. Rep. **3**, 3555 (2013).

[52] Z. H. Wang, L. Zhou, Y. Li and C. P. Sun, Phys. Rev. A **89**, 053813 (2014).

[53] W. Z. Jia, Y. W. Wang and Y.-x. Liu, Phys. Rev. A **96**, 053832 (2017).

[54] S. E. Harris, Phys. Rev. Lett. **62**, 1033 (1989).

[55] S. E. Harris and L. V. Hau, Phys. Rev. Lett. **82**, 4611 (1999).

[56] M. D. Lukin, Rev. Mod. Phys. **75**, 457 (2003).

[57] M. Fleischhauer, A. Imamoglu and J. P. Marangos, Rev. Mod. Phys. **77**, 633 (2005).

[58] A. Ask, Y.-L. L. Fang and A. F. Kockum, arXiv:2011.15077 (2020).